HHS Public Access

Author manuscript

Biochemistry. Author manuscript; available in PMC 2015 June 30.

Published in final edited form as:

Biochemistry. 2013 April 23; 52(16): 2705–2707. doi:10.1021/bi400280z.

The Hemophore HasA from *Yersinia pestis* ($HasA_{yp}$) Coordinates Hemin with a Single Residue, Tyr75, and with Minimal Conformational Change

Ritesh Kumar[‡], **Scott Lovell**[&], **Hirotoshi Matsumura**[€], **Kevin P. Battaile**[¶], **Pierre Moënne-Loccoz**[€], and **Mario Rivera**[†,*]

[‡]Center for Bioinformatics, University of Kansas, 2030 Becker Drive, Lawrence, Kansas 66047

[&]Protein Structure Lab, Del Shankel Structural Biology Center, University of Kansas, 2034 Becker Drive, Lawrence, Kansas 66047

[€]Division of Environmental & Biomolecular Systems, Institute of Environmental Health, Oregon Health and Science University, 20000 Northwest Walker Road, Beaverton, Oregon 97006-8921

[¶]IMCA-CAT, Hauptman Woodward Medical Research Institute, 9700 S. Cass Avenue, Bldg. 435A, Argonne, Illinois 60439

[†]Department of Chemistry, University of Kansas, 2030 Becker Drive, Lawrence, Kansas 66047

Abstract

Hemophores from *Serratia marcescens* ($HasA_{sm}$) and *Pseudomonas aeruginosa* ($HasA_p$) bind hemin between two loops, which harbor the axial ligands H32 and Y75. Hemin binding to the Y75 loop triggers closing of the H32 loop and enables binding of H32. Because *Yersinia pestis* HasA ($HasA_{yp}$) presents a Gln at position 32, we determined the structures of apo-and holo-$HasA_{yp}$. Surprisingly, the Q32 loop in apo-$HasA_{yp}$ is already in the closed conformation but no residue from the Q32 loop binds hemin in holo-$HasA_{yp}$. In agreement with the minimal reorganization between the apo-and holo-structures, the hemin on-rate is too fast to detect by conventional stopped-flow measurements.

Keywords

Hemophore; Heme; Hemin; *Yersinia pestis*; *Pseudomonas aeruginosa*; HasA

Although iron is important for many crucial biological functions, its chemical properties present unique challenges to living cells, which have to overcome the insolubility of Fe(III) and the toxicity of Fe(II) by sequestering iron in heme, iron-sulfur clusters or iron binding proteins. The very low concentrations of free iron in host cells pose significant challenges to

[*]**Corresponding Author** Telephone: (785) 864-4936. mrivera@ku.edu.

ASSOCIATED CONTENT

Supporting Information

Detailed experimental procedures. This material is available free of charge via the Internet at http://pubs.acs.org.

Accession codes

PDB entries 4JER (apo-$HasA_{yp}$ ^{tet}), 4JES (apo-$HasA_{yp}$ ^{hex}), 4JET (holo-$HasA_{yp}$)

pathogenic bacteria, which have evolved efficient strategies to scavenge iron, including secretion of hemophores, siderophores, hemolysins, proteases and cytotoxins (1, 2). Given that ~70% of total iron is bound to hemoglobin, heme is an important iron source. Thus, a strategy used by bacteria to acquire heme is the deployment of hemophores, which are outer membrane-exposed, or secreted proteins involved in the path of heme transfer from their location in the host to the bacterial cytosol (2, 3), where the macrocycle is degraded by heme-degrading enzymes to release the iron (1, 4, 5). The HasA-type hemophore was first identified in *Serratia marcescens* (6) and then shown to be conserved in several Gram negative pathogens including, *Pseudomonas aeruginosa*, *Pseudomonas fluorescens*, *Yersinia pestis*, *Yersinia pseudotuberculosis*, *Erwinia carotovora* and *Pectobacterium carotovorum* (7–11). Hemophores from *S. marcescens* ($HasA_{sm}$) (12, 13) and *P. aeruginosa* ($HasA_p$) (7, 14) have been structurally characterized in their apo-and heme-bound (holo) forms and found to be nearly identical. The hemin iron in holo-$HasA_p$ (and $HasA_{sm}$) is coordinated by H32 and Y75. Each axial ligand is harbored in a loop, termed either the H32 or Y75 loop. The main difference between the apo-and holo-structures is a large rearrangement of the H32 loop, which relocates H32 ~30 Å (Figure 1). Structural and spectroscopic studies carried out with WT and H32A $HasA_p$ (7, 15) showed that hemin loads onto the Y75 loop within a few milliseconds. Once hemin is loaded its proximal side is likely rapidly coordinated by Y75, while coordination by H32 is significantly slower (hundreds of milliseconds to second scale). In the structure of H32A holo-$HasA_p$ in complex with imidazole, hemin-iron is coordinated by Y75 and imidazole, the H32 loop is near the distal heme face and adopts a conformation very similar to that of WT holo-$HasA_p$; NMR studies suggest that this conformation is maintained in solution (7). These findings led to the conclusion that hemin loading onto the Y75 loop triggers closing of the H32 loop. Results from targeted molecular dynamic simulations allowed identification of motions that are likely important for transmitting the presence of heme in the Y75 loop to the H32 loop in order to initiate its closing (7).

Given the unusual His/Tyr coordination of the hemin-iron and the induced fit closing of the H32 loop upon hemin loading onto the Y75 loop of $HasA_p$ or $HasA_{sm}$, it is intriguing that H32 is not conserved amongst HasA proteins. Hemophore sequences from *Yersinia* species (Figure S1) contain a Gln at position 32 and do not have a His residue close in the sequence that could coordinate the hemin iron. These observations suggest that if the hemophore structures of *Yersinia* species are similar to $HasA_p$ and $HasA_{sm}$, the hemin iron would be axially coordinated by an unprecedented set of ligands, Q32 and Y75. In order to understand how the structures of hemophores compensate for the absence of H32, we carried out the structural characterization of the hemophore from *Yersinia pestis* KIM10+ ($HasA_{yp}$) in its heme-free (apo-) and heme-bound (holo-) forms. As will be shown below, unlike $HasA_p$ and $HasA_{sm}$, the structure of apo-$HasA_{yp}$ is in a closed conformation, and undergoes minimal rearrangement upon binding heme.

A synthetic gene coding for $HasA_{yp}$ was expressed in *E. coli* BL21-GOLD (DE3) cells. Purification yields a mixture of apo-and holo-proteins truncated at the C-terminus (Supporting Information). C-terminal cleavage of hemophores is common (11, 17) and may have functional relevance: The most abundant form of $HasA_p$ secreted by *P. aeruginosa* is

the truncated protein missing 15–21 C-terminal residues (18). In contrast, the most abundant form of $HasA_p$ secreted by quorum sensing-impaired mutants of *P. aeruginosa* is full-length $HasA_p$ (18). Consequently, the structural characterization of $HasA_p$ was carried out with truncated protein (14). Herein we report the structural characterization of C-terminus truncated $HasA_{yp}$.

The Q-32-bearing loop in apo-$HasA_{yp}$ is in the closed conformation

Tetragonal and hexagonal crystal forms were obtained from apo-$HasA_{yp}$. The tetragonal crystal form (apo-$HasA_{yp}{}^{tet}$), which has one molecule in the asymmetric unit, was refined to a resolution of 1.1 Å (Table S1 and Figure 2-A). Electron density was observed from S2 to M184, except for T48 and L49, which were not modeled. Apo-$HasA_{yp}$ exhibits the $\alpha + \beta$ fold characteristic of $HasA_p$ and $HasA_{sm}$ (12, 14), which is composed of a "β-sheet wall" of nine anti-parallel β-strands connected by hairpins and an "α-helix wall" composed of three α-helices and a 3_{10}-helix. The structure of the Y75 loop, extending from Y75 to F83, is identical to the Y75 loops in $HasA_p$ and $HasA_{sm}$. Interestingly, the loop bearing Q32, extending from N26 to S42, adopts a different conformation from that seen in apo-$HasA_p$ and apo-$HasA_{sm}$ (Figure 2-B). Its conformation is very similar to the "closed" conformation seen in the H32 loop of holo-$HasA_p$ and holo-$HasA_{sm}$. The closed loop conformation of the Q32 loop in apo-$HasA_{yp}{}^{tet}$ is also observed in the structure obtained from the hexagonal crystal form ($HasA_{yp}{}^{hex}$), which exhibits two molecules in the asymmetric unit and was refined to 1.6 Å resolution (Table S1, Figure S2-A). Both molecules in the asymmetric unit are nearly identical (C_α-RMSD = 0.76 Å), exhibit well-defined electron density for residues S2 to D180 and contain a PEG molecule between the Q32 and Y75 loops. Superposing the $HasA_{yp}{}^{tet}$ structure with the structures of molecules A and B of $HasA_{yp}{}^{hex}$ reveals near identical architectures (see Figure S2-B), except for the apparent absence of PEG or other exogenous molecules between the Q32 and Y75 loops of apo- $HasA_{yp}{}^{tet}$.

The structures of apo- and holo-$HasA_{yp}$ are nearly identical

The crystal structure of holo-$HasA_{yp}$ was solved to a resolution of 2.2 Å (Table S1 and Figure 2-C). Well-defined electron density was traced from S2 to D180 for each of the 10 molecules in the asymmetric unit; superposing all ten chains results in a C_α-RMSD = 0.50 Å. Figure 2 illustrates the surprising observation that unlike $HasA_p$ or $HasA_{sm}$, the Q32-loop in $HasA_{yp}$ does not change conformation upon binding hemin (C_α-RMSD = 0.56 Å). As in the previously characterized hemophores, the hemin iron in $HasA_{yp}$ is coordinated by Y75, which also forms a hydrogen bond (2.7 Å) with the N_δ of H81 (H83 in $HasA_{sm}$ and $HasA_p$). Despite the similar coordinating environment of the proximal binding site, the environment of the distal site in $HasA_{yp}$ is distinct (Figure 2-D and E) in that the 6^{th} coordination site is not occupied by a protein-provided ligand. Note that Q32, which we hypothesized may coordinate the hemin iron, is located approximately 14 Å away (C_α) from the heme iron, in a position very similar to the one it occupies in the apo-form. Q32 is clearly not part of the heme-binding pocket. The most significant change in the Q32 loop upon hemin binding is the relocation of the R40 side chain (Figure 3). This small reorganization protects the hemin distal face immediately after it binds to $HasA_{yp}$, a situation that contrasts with apo-$HasA_p$ or apo-$HasA_{sm}$, where the hemin distal face is exposed to the aqueous environment prior to

closing of the H32 loop. The Q32-loop of $HasA_{yp}$ is 3-residues shorter than the H32 loop of $HasA_p$ and $HasA_{sm}$ (Figure S1 and Figure S3) which may decrease the conformational flexibility of the Q32 loop. This issue is currently under investigation in our laboratories.

Electron density immediately above the hemin iron was best modeled as a chloride ion (Figure 3). The modeled Cl^- is not within binding distance of Fe(III) (Fe-Cl = 2.8 Å). In contrast, the resonance Raman and EPR spectra show that in solution the heme iron(III) in holo-$HasA_{yp}$ adopts a 6-coordinate high-spin configuration (Figure S4). Although attempts to detect Fe(III)-Cl and Fe(III)-OH stretching frequencies were unsuccessful we presume that the sixth ligand might be a solvent molecule and/or a loosely bound chloride ion. Because HasA sequences with Q32 contain R40 but those with H32 do not (Figure S1), we hypothesize that R40 may stabilize the chloride ion observed in the holo-$HasA_{yp}$ structure. In contrast to the large differences observed in the H32 loop, the structure of the Y75 loop is conserved amongst the three hemophores (Figure S5). As pointed out previously (7) the proximal loop forms a conserved hydrophobic surface for hemin to interact with the hemophore. Accordingly, hemin binding to $HasA_{yp}$ causes minimal changes to the Y75 loop; the largest change is a rearrangement of the F83 side chain to accommodate the incoming hemin (Figure 3).

$HasA_{yp}$ loads hemin from solution faster than $HasA_p$

Stopped-flow experiments reveal that hemin capture by apo-$HasA_{yp}$ is complete within the millisecond deadtime of the apparatus and is thus much faster than in apo-$HasA_p$ (Figure S6). These observations support the idea that apo-$HasA_{yp}$ adopts a closed configuration in solution and that minimal reorganization occurs upon binding hemin. This distinctive behavior of $HasA_{yp}$ is likely to also affect hemin transfer to the receptor protein, which in *S. marcescens* is thought to modulate hemin binding affinity to $HasA_{sm}$ via interaction with the H32 loop (19).

Supplementary Material

Refer to Web version on PubMed Central for supplementary material.

ACKNOWLEDGMENTS

Use of the Advanced Photon Source was supported by the U.S. Department of Energy, Office of Sciences, under Contact No. DE-AC02-06CH11357. Use of the IMCA-CAT beamline 17-ID at the Advanced Photon Source was supported by the companies of the Industrial Macromolecular Crystallography Association through a contract with Hauptman-Woodward Medical Research Institute. Use of the KU COBRE-PSF Protein Structure Laboratory was supported by grants from the National Center for Research Resources (5P20RR017708-10) and the National Institute of General Medical Sciences (8 P20 GM103420-10) from the National Institutes of Health. M.R. thanks David R. Benson for insightful discussion.

Funding

This study was supported by grants from the National Science Foundation (M.R., MCB1158469 and MCB 0818488; PML MCB0811888) and by a fellowship from the Japan Society for the Promotion of Science (H.M.).

REFERENCES

1. Benson DR, Rivera M. Met. Ions Life Sci. 2013; 12:279–332. [PubMed: 23595676]

2. Wandersman C, Delepelaire P. Mol Microbiol. 2012; 85:618–631. [PubMed: 22715905]
3. Tullius MV, Harmston CA, Owens CP, Chim N, Morse RP, McMath LM, Iniguez A, Kimmey JM, Sawaya MR, Whitelegge JP, Horwitz MA, Goulding CW. P Natl Acad Sci USA. 2011; 108:5051–5056.
4. Smith AD, Wilks A. Current topics in membranes. 2012; 69:359–392. [PubMed: 23046657]
5. Skaar EP, Gaspar AH, Schneewind O. J. Biol. Chem. 2004; 279:436–443. [PubMed: 14570922]
6. Létoffé S, Ghigo JM, Wandersman C. Proc. Natl. Acad. SciU.SA. 1994; 91:9876–9880.
7. Jepkorir G, Rodriguez JC, Rui H, Im W, Lovell S, Battaile KP, Alontaga AY, Yukl ET, Moenne-Loccoz P, Rivera M. J Am Chem Soc. 2010; 132:9857–9872. [PubMed: 20572666]
8. Cescau S, Cwerman H, Letoffe S, Delepelaire P, Wandersman C, Biville F. Biometals. 2007; 20:603–613. [PubMed: 17268821]
9. Rossi MS, Fetherston JD, Letoffe S, Carniel E, Perry RD, Ghigo JM. Infect Immun. 2001; 69:6707–6717. [PubMed: 11598042]
10. Ochsner UA, Johnson Z, Vasil ML. Microbiology. 2000; 146(Pt 1):185–198. [PubMed: 10658665]
11. Letoffe S, Redeker V, Wandersman C. Mol Microbiol. 1998; 28:1223–1234. [PubMed: 9680211]
12. Arnoux P, Haser R, Izadi N, Lecroisey A, Delepierre M, Wandersman C, Czjzek M. Nat Struct Biol. 1999; 6:516–520. [PubMed: 10360351]
13. Wolff N, Izadi-Pruneyre N, Couprie J, Habeck M, Linge J, Rieping W, Wandersman C, Nilges M, Delepelairre P, Lecroisey A. J. Mol. Biol. 2008; 376:517–525. [PubMed: 18164722]
14. Alontaga AY, Rodriguez JC, Schonbrunn E, Becker A, Funke T, Yukl ET, Hayashi T, Stobaugh J, Moenne-Loccoz P, Rivera M. Biochemistry. 2009; 48:96–109. [PubMed: 19072037]
15. Yukl ET, Jepkorir G, Alontaga AY, Pautsch L, Rodriguez JC, Rivera M, Moenne-Loccoz P. Biochemistry. 2010; 49:6646–6654. [PubMed: 20586423]
16. Krissinel E, Henrick K. Acta Crystallogr D Biol Crystallogr. 2004; 60:2256–2268. [PubMed: 15572779]
17. Letoffe S, Ghigo JM, Wandersman C. J Bacteriol. 1994; 176:5372–5377. [PubMed: 8071214]
18. Arevalo-Ferro C, Hentzer M, Reil G, Gorg A, Kjelleberg S, Givskov M, Riedel K, Eberl L. Environ Microbiol. 2003; 5:1350–1369. [PubMed: 14641579]
19. Krieg S, Huche F, Diederichs K, Izadi-Pruneyre N, Lecroisey A, Wandersman C, Delepelaire P, Welte W. P Natl Acad Sci USA. 2009; 106:1045–1050.

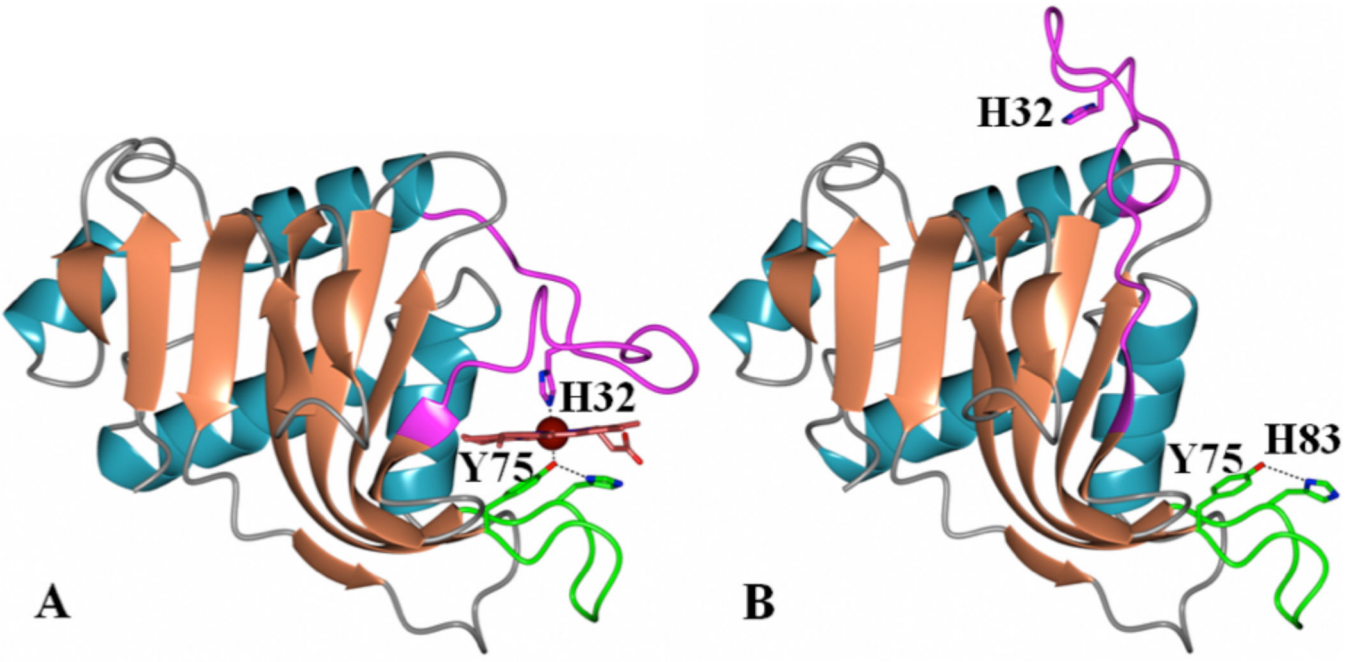

Figure 1.

Structure of (A) holo-HasA$_p$ (PDB: 3ELL) and (B) apo-HasA$_p$ (PDB: 3MOK) showing the proximal (Y75) and distal (H32) ligands. The Y75 loop is shown in green, the H32 loop in magenta and the heme in red. Heme loads onto the Y75 loop, triggers closure of the H32 loop and enables H32 to coordinate the heme iron.

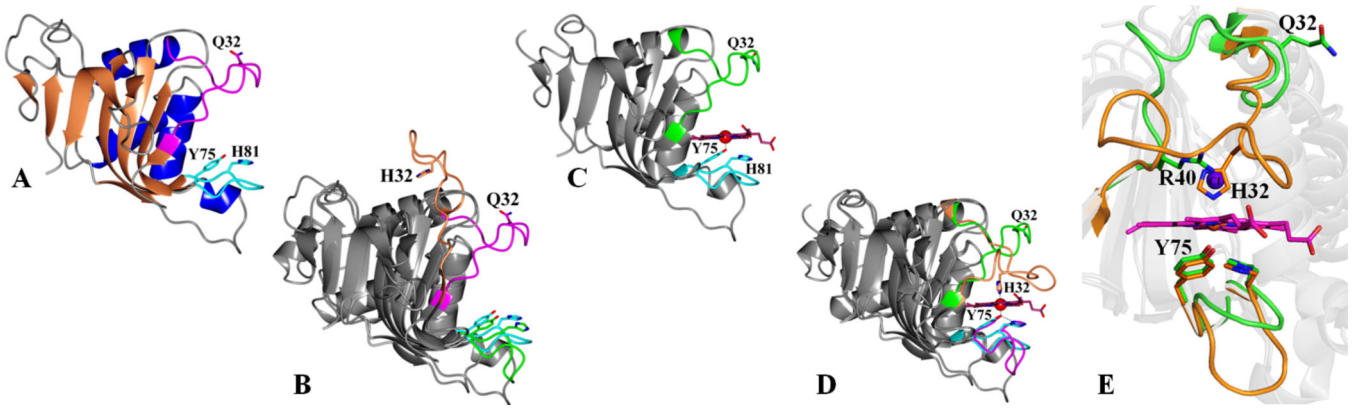

Figure 2.

(**A**) Structure of apo-HasA$_{yp}$ ^{tet} with the Q32 loop shown in magenta and the Y75 loop in cyan; Q32, Y75 and H81 are shown in sticks. (**B**) Superimposed structures of apo-HasA$_{p}$ (PDB ID: 3MOK) and apo-HasA$_{yp}$ ^{tet} where the H32 loop in apo-HasA$_{p}$ is shown in coral and the Q32 loop in apo-HasA$_{yp}$ ^{tet} in magenta. (**C**) The structure of holo-HasA$_{yp}$ is very similar to that of apo-HasA$_{yp}$; the Q32 loop is in green and the Y75 loop in cyan. (**D**) Superposition of holo-HasA$_{yp}$ and holo-HasA$_{p}$ (PDB ID: 3ELL) structures. The hemin iron in HasA$_{p}$ is coordinated by Y75 and H32, whereas in holo-HasA$_{yp}$ it is coordinated by Y75 (also see Figure 3). (E) Zoomed-in view comparing the heme-binding pockets of holo-HasA$_{yp}$ (green) and holo-HasA$_{p}$ (orange); a chloride ion (purple sphere) in the distal pocket of HasA$_{yp}$ is in the position occupied by the side chain of H32 in holo-HasA$_{p}$ and holo-HasA$_{sm}$. Structures were superimposed using the program Superpose (16).

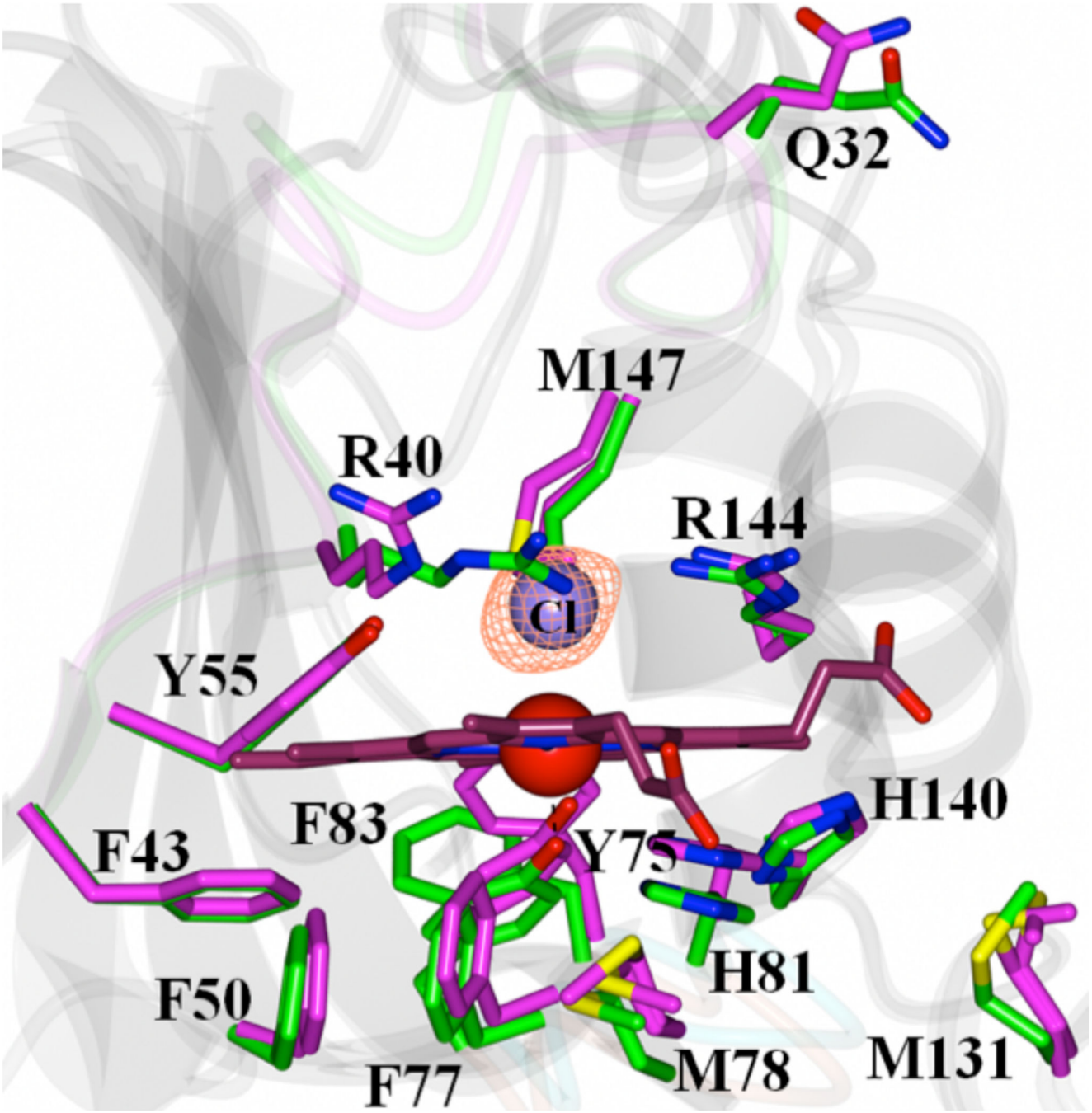

Figure 3.

View of the heme-binding pocket in the superimposed structures of apo-$HasA_{yp}$ ^{tet} and holo-$HasA_{yp}$ illustrate the minor structural differences between apo-(magenta) and holo-(green) $HasA_{yp}$. The distal site in the holo protein is coordinated by a chloride ion; the F_o-F_c omit map contoured at 3 σ is shown in mesh representation.